EUROPEAN ORGANIZATION FOR NUCLEAR RESEARCH (CERN)

CERN-EP-2024-281
LHCb-PAPER-2024-043
November 23, 2024

Study of Λ_b^0 and Ξ_b^0 decays to $\Lambda h^+ h'^-$ and evidence for CP violation in $\Lambda_b^0 \to \Lambda K^+ K^-$ decays

LHCb collaboration[†]

Abstract

A study of Λ_b^0 and Ξ_b^0 decays to $\Lambda h^+ h'^-$ $(h^{(\prime)} = \pi, K)$ is performed using pp collision data collected by the LHCb experiment during LHC Runs 1–2, corresponding to an integrated luminosity of $9\,\text{fb}^{-1}$. The branching fractions for these decays are measured using the $\Lambda_b^0 \to \Lambda_c^+(\to \Lambda\pi^+)\pi^-$ decay as control channel. The decays $\Lambda_b^0 \to \Lambda\pi^+\pi^-$ and $\Xi_b^0 \to \Lambda K^-\pi^+$ are observed for the first time. For decay modes with sufficient signal yields, CP asymmetries are measured in the full and localized regions of the final-state phase space. Evidence is found for CP violation in the $\Lambda_b^0 \to \Lambda K^+ K^-$ decay, interpreted as originating primarily from an asymmetric $\Lambda_b^0 \to N^{*+} K^-$ decay amplitude. The measured CP asymmetries for the other decays are compatible with zero.

Submitted to Phys. Rev. Lett.

[†]Authors are listed at the end of this paper.

In the Standard Model (SM) of particle physics, symmetry breaking under the combined charge-conjugation and parity transformations (CP violation) originates from a complex phase within the Cabibbo–Kobayashi–Maskawa (CKM) matrix [1]. To date, all observed CP violation phenomena align with the CKM mechanism. However, the amount of CP violation in the SM is insufficient to explain the observed matter-antimatter imbalance in the Universe [2], motivating further study of CP violation and searches for possible new sources beyond the SM contributions.

While the breaking of CP symmetry has been established and extensively studied in K, B and D meson decays, it has never been observed in any baryon decay. The BESIII experiment has conducted comprehensive searches for CP violation in light hyperon decays, including studies of decay rates and parameters, finding no evidence for CP violation [3]. Searches for CP violation have been pursued by LHCb in bottom-baryon decays, including $\Lambda_b^0 \to K_S^0 p\pi^-$ [4],[1] $\Lambda_b^0 \to J/\psi p\pi^-$ [5] $\Lambda_b^0 \to ph^-h'^+h''^-$ [6–10], $\Lambda_b^0 \to \Lambda K^+K^-$, $\Lambda_b^0 \to \Lambda K^+\pi^-$ [11], $\Lambda_b^0 \to pK^-\mu^+\mu^-$ [12], $\Lambda_b^0 \to ph^-$ [13], $\Xi_b^- \to pK^-K^-$ [14], $\Lambda_b^0 \to \Lambda\gamma$ [15], $\Lambda_b^0 \to \Lambda\phi$ [16], and charm-baryon decays such as $\Lambda_c^+ \to ph^+h^-$ [17] and $\Xi_c^+ \to pK^-\pi^+$ [18], where $h, h', h'' = \pi$ or K throughout this Letter. These measurements are statistically limited, as most of them use only data collected during LHC Run 1 (2011–2012). Further investigation of CP violation in baryon decays may shed new light on the dynamics of weak decays in the baryon sector and provide a better picture of CP violation originating from quark transitions.

In three-body charmless B-meson decays, $B \to h^+h'^-h''^+$, large CP violation up to 75% is observed in localized regions of phase space, for example in the low K^+K^-, low $\pi^+\pi^-$ and high $\pi^+\pi^-$ mass regions [19–21]. These results suggest that resonance interactions and $\pi^+\pi^- \leftrightarrow K^+K^-$ S-wave rescattering play an important role in the generation of strong phases needed for direct CP violation, and motivate further studies of Λ_b^0 and Ξ_b^0 decays to $\Lambda h^+h'^-$ final states, which are governed by similar dynamics in the SM.

Quasi-two-body charmless Λ_b^0 decays, $\Lambda_b^0 \to \Lambda\omega/\Lambda\phi/\Lambda\rho$, have been studied with the QCD factorization approach and their CP violation is predicted to be in the range 0% to 4% with branching fractions at the level of 10^{-7} [22–25]. The generalized factorization approach (GFA), considering part of the nonfactorizable sources by introducing an effective color number N_c, gives similar CP asymmetry predictions but the branching fractions are predicted to be approximately 10^{-6} [26, 27]. For the $\Lambda_b^0 \to N^{*+}\pi^-$ decay, the CP asymmetry is predicted to be in the range from -4% to 6% [28]. In a previous LHCb study, the $\Lambda_b^0 \to \Lambda K^+K^-$ and $\Lambda_b^0 \to \Lambda K^+\pi^-$ decays were observed with the Run 1 sample [11], where the first evidence for $\Lambda_b^0 \to \Lambda\pi^+\pi^-$ was established and the CP asymmetries for these decays were found to be compatible with zero.

Further higher-precision measurements of CP asymmetries and branching fractions of Λ_b^0 and Ξ_b^0 decays to $\Lambda h^+h'^-$ final states offer stringent tests of these models and provide a foundation to study other quasi-two-body decays that have not been considered before.

This Letter reports the measurements of branching fractions and CP violation parameters for charmless decays of Λ_b^0 and Ξ_b^0 baryons into the final states $\Lambda K^\pm\pi^\mp$, ΛK^+K^-, and $\Lambda\pi^+\pi^-$, among which the suppressed modes $\Lambda_b^0 \to \Lambda K^-\pi^+$ and $\Xi_b^0 \to \Lambda K^+\pi^-$ are not considered. The study is performed based on proton-proton (pp) collision data collected with the LHCb detector during LHC Runs 1–2 (2011–2018) at center-of-mass energies of 7, 8 and 13 TeV and corresponding to an integrated luminosity of 9 fb^{-1}. The

[1] The inclusion of charge-conjugated processes is implied throughout the article if not specified.

$\Lambda_b^0 \to \Lambda_c^+(\to \Lambda\pi^+)\pi^-$ decay is used as control channel for both the branching fraction and CP-violation measurements to reduce systematic uncertainties.

The LHCb detector is a single-arm forward spectrometer covering the pseudorapidity range $2 < \eta < 5$, described in detail in Refs. [29, 30]. It is designed specifically for the study of particles containing b or c quarks. Of particular relevance for this analysis is the tracking system, comprising silicon-strip stations upstream and straw drift tube stations downstream of a 4 T m dipole magnet [31, 32], and the Ring-Imaging Cherenkov (RICH) [33] detectors used for the particle identification (PID) [34, 35], whose performance of simulated samples is calibrated to match that evaluated with high-yield decay modes in data. The Λ_b^0/Ξ_b^0 decays are selected by an online trigger system which consists of a hardware stage followed by a software stage [35, 36]. The hardware trigger is based on information from the calorimeter and muon systems. The software trigger applies full event reconstruction, selecting events with a two-, three- or four-track secondary vertex with a significant displacement from any primary pp interaction vertex. Simulated $\Lambda_b^0/\Xi_b^0 \to \Lambda h^+h'^-$ decays are used to model the effects of the detector acceptance and imposed selection requirements, and the signal mass distributions. In the simulation, samples are generated with PYTHIA [37], EVTGEN [38], PHOTOS [39] and the GEANT4 toolkits [40] as described in Ref. [41].

In the offline selection, tracks identified as a proton and a pion are used to form a Λ candidate, which is further combined with a pair of oppositely charged hadrons identified as a pion or kaon to form a Λ_b^0/Ξ_b^0 candidate. Backgrounds from specific narrow resonances including K_S^0, D^0, Λ_c^+, Ξ_c^+, J/ψ and χ_{c0} hadrons formed by combinations of tracks from the final state particles of Λ_b^0/Ξ_b^0 candidates are removed by vetoing in the relevant mass spectra. Further discrimination of signal from background is achieved through a Boosted Decision Tree (BDT) classifier [42, 43], using a combination of kinematic and topological variables as inputs. The BDT classifier is trained with simulated $\Lambda_b^0 \to \Lambda\pi^+\pi^-$ decays as the signal, and using the data sample in the mass region $m(\Lambda\pi^+\pi^-) \in [5800, 6100]\,\text{MeV}/c^2$ as the background. Requirements on the BDT response and PID of final-state tracks are optimized and applied simultaneously to maximize the figure-of-merit, defined as $N_S/\sqrt{N_S + N_B}$ ($N_S/(\sqrt{N_B} + 2.5)$) for the Λ_b^0 (Ξ_b^0) decays. Here N_S and N_B are the signal and background yields in the Λ_b^0 (Ξ_b^0) signal region, defined as a $\pm 50\,\text{MeV}/c^2$ mass window around the known Λ_b^0 (Ξ_b^0) mass [44]. The PID requirements help to reduce combinatorial background and cross-feeds from other signal decays and from B-meson decays. The contributions from B-meson decays are suppressed to a negligible level.

The $\Lambda h^+h'^-$ mass distributions after all selections are shown in Fig. 5 of the End Matter, together with fit projections. The obtained signal yields are summarized in Table 1, extracted using a simultaneous unbinned maximum-likelihood fit to all the $\Lambda h^+h'^-$ mass distributions, where the two CP conjugate states are combined. The signal component in the corresponding $\Lambda h^+h'^-$ mass distribution is modeled by the sum of two Crystal Ball (CB) functions [45], with tail parameters fixed from simulation. The distributions of cross-feeds from other signal decays due to misidentified h^+ or h'^- hadrons are obtained from simulation, and their yields are constrained to the respective yields of the correctly reconstructed signals multiplied by the experimental efficiencies evaluated from simulation. The decay $\Lambda_b^0 \to \Lambda h^+h'^-\gamma/\pi^0$, with γ/π^0 not reconstructed, is modeled by an ARGUS function [46] convolved by a Gaussian distribution for the experimental resolution. The shape parameters of ARGUS function are constrained from simulation. The combinatorial background is modeled by an exponential function. For CP-violation measurements, the

Table 1: Signal yield and (upper limit of) *CP*-averaged branching fraction ($\mathcal{B}$) for each decay mode. The uncertainties are statistical, systematic and due to the branching fraction of the control mode. The yield for the control mode is also shown.

Decay	Yield	$\mathcal{B}$ $(\times 10^{-6})$
$\Lambda_b^0 \to \Lambda\pi^+\pi^-$	$(6.4 \pm 0.4) \times 10^2$	$5.3 \pm 0.4 \pm 0.5 \pm 0.5$
$\Lambda_b^0 \to \Lambda K^+\pi^-$	$(6.18 \pm 0.32) \times 10^2$	$4.6 \pm 0.2 \pm 0.4 \pm 0.5$
$\Lambda_b^0 \to \Lambda K^+K^-$	$(1.92 \pm 0.05) \times 10^3$	$10.7 \pm 0.3 \pm 0.4 \pm 1.1$
$\Xi_b^0 \to \Lambda\pi^+\pi^-$	$(5.6 \pm 2.7) \times 10^1$	$11.0 \pm 2.6 \pm 1.4 \pm 3.8$
$\Xi_b^0 \to \Lambda K^-\pi^+$	$(1.19 \pm 0.15) \times 10^2$	$10.4 \pm 1.4 \pm 1.2 \pm 3.5$
$\Xi_b^0 \to \Lambda K^+K^-$	$(1.2 \pm 0.9) \times 10^1$	< 2.4 (2.8) at 90% (95%) CL
$\Lambda_b^0 \to \Lambda_c^+(\to \Lambda\pi^+)\pi^-$	$(5.25 \pm 0.07) \times 10^3$	—

signal and background parameters are shared between baryon and antibaryon decays.

Using Wilks' theorem [47], the statistical significances of the $\Lambda_b^0 \to \Lambda\pi^+\pi^-$ and $\Xi_b^0 \to \Lambda K^-\pi^+$ decays are measured to be more than $10\,\sigma$, giving the first observation of these decays. The significance of the $\Xi_b^0 \to \Lambda\pi^+\pi^-$ decay is determined to be $4\,\sigma$, while that of the $\Xi_b^0 \to \Lambda K^+K^-$ decay is about $1.7\,\sigma$.

The branching-fraction ($\mathcal{B}$) ratio of a signal decay to that of the control mode is measured according to

$$\frac{\mathcal{B}\,(\Lambda_b^0/\Xi_b^0 \to \Lambda h^+h'^-)}{\mathcal{B}\,(\Lambda_b^0 \to \Lambda_c^+\,(\to \Lambda\pi^+)\,\pi^-)} = \frac{N_{\Lambda_b^0/\Xi_b^0 \to \Lambda h^+h'^-}}{N_{\Lambda_b^0 \to \Lambda_c^+(\to\Lambda\pi^+)\pi^-}} \times \frac{\epsilon_{\Lambda_b^0 \to \Lambda_c^+(\to\Lambda\pi^+)\pi^-}}{\epsilon_{\Lambda_b^0/\Xi_b^0 \to \Lambda h^+h'^-}} \times \frac{f_{\Lambda_b^0}}{f_{\Lambda_b^0/\Xi_b^0}}\,, \tag{1}$$

where N and ϵ are the yield and efficiency for the considered decay, respectively, and the final factor is the ratio of b-quark fragmentation fractions [48, 49]. The yields are determined through the fit to data while the efficiencies are determined from simulation. In the simulation the p_{T} and rapidity distributions of the Λ_b^0 baryon [50], as well as the Dalitz plot of the Λ_b^0/Ξ_b^0 decays, are corrected to match those in data. The efficiencies are at the level of 10^{-4}, with the efficiency ratio in the range 0.8–2.9 depending on the signal channel. For Ξ_b^0 decays, due to the limited data sample, the p_{T} and rapidity are not corrected and a 10% systematic uncertainty is assigned to the efficiency.

The branching-fraction results are summarized in Table 1, where the uncertainties are statistical, systematic and due to the uncertainty of the control channel branching fraction [48, 51]. As no significant contribution from the $\Xi_b^0 \to \Lambda K^+K^-$ decay is found, upper limits are determined on its branching fraction at 90% and 95% confidence levels (CL), by integrating the positive side of the profile likelihood [52].

Four channels with sufficiently high yields, including three Λ_b^0 decay modes and the $\Xi_b^0 \to \Lambda K^-\pi^+$ decay mode, are selected for further investigation of *CP* violation. The *CP* asymmetry of the decay to a final state f is defined as

$$\mathcal{A}^{CP}(\Lambda_b^0/\Xi_b^0 \to f) \equiv \frac{\Gamma(\Lambda_b^0/\Xi_b^0 \to f) - \Gamma(\overline{\Lambda}_b^0/\overline{\Xi}_b^0 \to \overline{f})}{\Gamma(\Lambda_b^0/\Xi_b^0 \to f) + \Gamma(\overline{\Lambda}_b^0/\overline{\Xi}_b^0 \to \overline{f})}, \tag{2}$$

where Γ is the partial decay rate defined without inclusion of its charge-conjugate process. The raw asymmetry of signal yields between baryon and antibaryon decays, denoted as $\mathcal{A}^{CP}_{\mathrm{raw}}$, is first extracted directly from the mass fits. This is then corrected to account

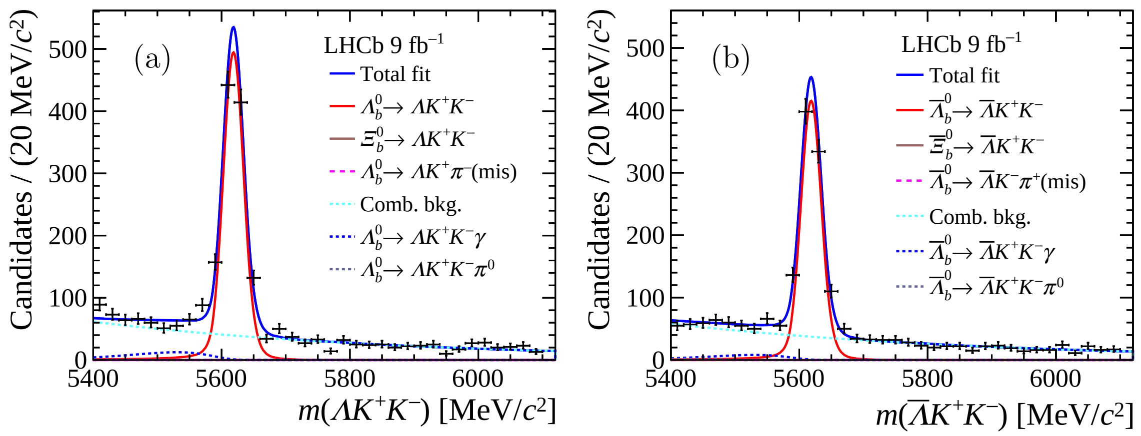

Figure 1: Mass distributions of (a) $\Lambda_b^0 \to \Lambda K^+ K^-$ and (b) $\overline{\Lambda}_b^0 \to \overline{\Lambda} K^+ K^-$ decays, with the fit projections.

for two factors: the asymmetry of the baryon and antibaryon production rates, $A_{\rm P}$, and the asymmetry of the final-state detection and selection efficiencies, $A_{\rm exp}$. To reduce systematic uncertainties, the difference between the CP asymmetry of each signal decay and the $\Lambda_b^0 \to \Lambda_c^+(\Lambda\pi^+)\pi^-$ decay, $\Delta\mathcal{A}^{CP}$, is measured. Assuming there is no CP violation for the control mode, valid within the experimental uncertainties of this analysis, $\Delta\mathcal{A}^{CP}$ gives the measurement of the CP asymmetry for the signal decay.

The Λ_b^0 production asymmetries in pp collisions at $\sqrt{s} = 7\,\text{TeV}$ and $8\,\text{TeV}$ have previously been measured at LHCb [13], but there is no equivalent measurement yet at $\sqrt{s} = 13\,\text{TeV}$. As the Λ_b^0 production asymmetry is expected to be smaller at higher energies and mostly cancels between the signal and control channel, the $A_{\rm P}$ measured for $\sqrt{s} = 8\,\text{TeV}$ is used for the $\Delta\mathcal{A}^{CP}(\Lambda_b^0)$ measurements at $\sqrt{s} = 13\,\text{TeV}$. Assuming isospin symmetry between the Ξ_b^0 and Ξ_b^- cross-sections in pp collisions, the Ξ_b^0 production asymmetry is taken to be the same as that of the Ξ_b^- baryon, which has been measured by the LHCb experiment [49]. The detection asymmetry encompasses the asymmetries in the final-state reconstruction, the trigger selection and the PID selection. The reconstruction asymmetries for pions, kaons and protons have been measured as a function of particle momenta using control samples of $D^+ \to K^0_S\pi^+$, $D^+ \to K^-\pi^+\pi^+$, $D^{*+} \to D^0(\to K^-\pi^+\pi^+\pi^-)\pi^+$ decays [53], and simulated samples of $\Lambda_b^0 \to \Lambda_c^+(\to pK^-\pi^+)\mu^-\overline{\nu}_\mu$ decays [13]. The detection asymmetry for each final-state particle is then weighted by its momentum distribution in the signal and control modes to get an averaged result, accounting for the kinematics of both modes. The PID and trigger selection asymmetries are obtained in a similar way using data [34,35]. The largest detection asymmetry, due to proton reconstruction, mostly cancels between the signal and control modes. These correction terms $\Delta A_{\rm P}$ and $\Delta A_{\rm exp}$ are shown in Table 3 in the End Matter, and are all consistent with zero for Λ_b^0 decays with uncertainties around 0.002 and 0.010, respectively. The $\Delta\mathcal{A}^{CP}$ quantities, integrated

Table 2: Definitions of the resonance-dominated regions and the corresponding $\Delta\mathcal{A}^{CP}$ values. The symbol f represents multiple resonances at low $\pi^+\pi^-$ mass.

Channel	$m(h^+h'^-)$	$m(\Lambda h^+)$	$\Delta\mathcal{A}^{CP}$
$\Lambda_b^0 \to \Lambda\phi\,(\to K^+K^-)$	$< 1.10\,\text{GeV}/c^2$	—	$0.150 \pm 0.055 \pm 0.021$
$\Lambda_b^0 \to N^{*+}(\to \Lambda K^+)K^-$	$> 2.20\,\text{GeV}/c^2$	$< 2.90\,\text{GeV}/c^2$	$0.165 \pm 0.048 \pm 0.017$
$\Lambda_b^0 \to N^{*+}(\to \Lambda K^+)\pi^-$	—	$< 2.30\,\text{GeV}/c^2$	$-0.078 \pm 0.051 \pm 0.027$
$\Lambda_b^0 \to \Lambda f\,(\to \pi^+\pi^-)$	$< 1.70\,\text{GeV}/c^2$	—	$0.088 \pm 0.069 \pm 0.021$

over the phase space, are measured for the four decays to be

$$\begin{aligned}
\Delta\mathcal{A}^{CP}\left(\Lambda_b^0 \to \Lambda\pi^+\pi^-\right) &= -0.013 \pm 0.053 \pm 0.018, \\
\Delta\mathcal{A}^{CP}\left(\Lambda_b^0 \to \Lambda K^+\pi^-\right) &= -0.118 \pm 0.045 \pm 0.021, \\
\Delta\mathcal{A}^{CP}\left(\Lambda_b^0 \to \Lambda K^+K^-\right) &= 0.083 \pm 0.023 \pm 0.016, \\
\Delta\mathcal{A}^{CP}\left(\Xi_b^0 \to \Lambda K^-\pi^+\right) &= 0.27 \pm 0.12 \pm 0.05,
\end{aligned}$$

where the first uncertainties are statistical and the second are systematic. The $\Delta\mathcal{A}^{CP}$ measurement for the $\Lambda_b^0 \to \Lambda K^+K^-$ decay has a significance of $3.1\,\sigma$ based on the negative log-likelihood method [54], accounting for both statistical and systematic uncertainties. This significance is confirmed by using ensembles of pseudoexperiments.

The mass distributions of $\Lambda_b^0 \to \Lambda K^+K^-$ for both baryon and antibaryon decays, with fit results also plotted, are shown in Fig. 1 where a clear difference in signal yields between Λ_b^0 and $\overline{\Lambda}_b^0$ decays can be seen. The decay is dominated by intermediate $N^{*+}(\to \Lambda K^+)$ or $\phi(\to K^+K^-)$ resonances, as can be seen in the $\Lambda_b^0 \to \Lambda K^+K^-$ Dalitz plot of Fig. 2 (a), where background contributions are subtracted using the *sPlot* technique [55]. To investigate whether these resonances are the source of the *CP* asymmetry, separate $\Delta\mathcal{A}^{CP}$ measurements are performed within these two resonance-dominated regions. In the region dominated by the N^{*+} resonance, the asymmetry is determined to be $\Delta\mathcal{A}^{CP} = 0.165 \pm 0.048 \pm 0.017$, which differs from zero by $3.2\,\sigma$. The mass distributions of the $\Lambda_b^0 \to \Lambda K^+K^-$ and $\overline{\Lambda}_b^0 \to \overline{\Lambda} K^+K^-$ decays and their fit projections, within the region, are shown in Fig. 3, demonstrating the difference between Λ_b^0 and $\overline{\Lambda}_b^0$ yields. The *CP* asymmetry in the ϕ region is consistent with zero. A possible variation of the *CP* asymmetry across the Dalitz plot is also studied in 10 equally populated Dalitz bins defined using an adaptive binning scheme. The results are consistent with *CP* symmetry.

The significances for *CP* violation in $\Lambda_b^0 \to \Lambda K^+\pi^-$, $\Lambda_b^0 \to \Lambda\pi^+\pi^-$ and $\Xi_b^0 \to \Lambda K^-\pi^+$ decays are $2.4\,\sigma$, $0.2\,\sigma$ and $2.1\,\sigma$, respectively. Further searches for *CP* violation are also performed for the two Λ_b^0 decays both in resonance-dominated regions (see Fig. 2 (b, c) and Table 2) and with an adaptive binning scheme. The results are all consistent with *CP* symmetry. For the Ξ_b^0 decays, no localized *CP* asymmetry searches are performed due to the low signal yields.

Cross-checks are performed to investigate the stability of the branching fraction and $\Delta\mathcal{A}^{CP}$ measurements. For the global asymmetries and branching fractions, results are obtained in different data-taking periods, as well as with different magnet polarities, and are found to be consistent. For the measurements in different resonance-dominated regions, alternative definitions of the mass regions are used, and similar results as the nominal ones are obtained.

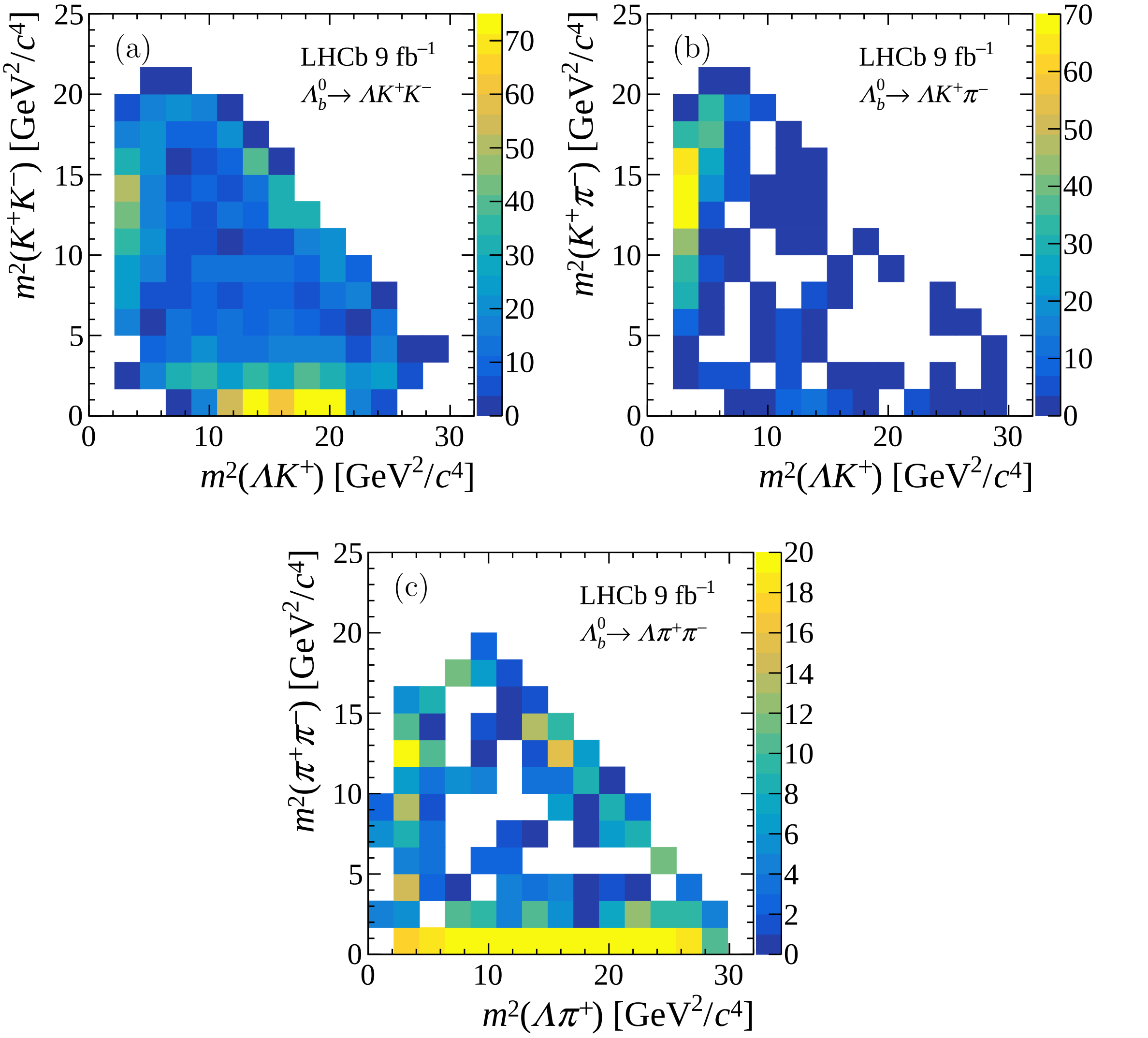

Figure 2: Dalitz plots of (a) $\Lambda_b^0 \to \Lambda K^+ K^-$, (b) $\Lambda_b^0 \to \Lambda K^+ \pi^-$, (c) $\Lambda_b^0 \to \Lambda \pi^+ \pi^-$ decays. Background contributions are subtracted using the *sPlot* technique. The coordinates are calculated after a kinematic fit which constrains the Λ_b^0 and Λ baryon masses to their known values [44].

Various sources of systematic uncertainties on the branching fraction and $\Delta\mathcal{A}^{CP}$ measurements are considered. The uncertainty due to the imperfect modelling of the mass distributions is evaluated by using alternative models for each component, including an Hypatia function [56] for the signal model and a second-order polynomial function for the combinatorial background. For the $\Delta\mathcal{A}^{CP}$ measurements, an additional uncertainty arises from using shared fit parameters for baryon and antibaryon decays. This is assessed by removing this constraint and assigning the resulting $\Delta\mathcal{A}^{CP}$ shifts as systematic uncertainties. The systematic uncertainty from the efficiency ratio has several contributions. The first contribution arises from the finite size of simulation samples, which is propagated to the branching fraction and $\Delta\mathcal{A}^{CP}$ measurements using pseudoexperiments. Another contribution is due to the robustness of efficiency corrections, which are studied in alternative scenarios. For example, the effect of the vetoing of charm hadrons is studied

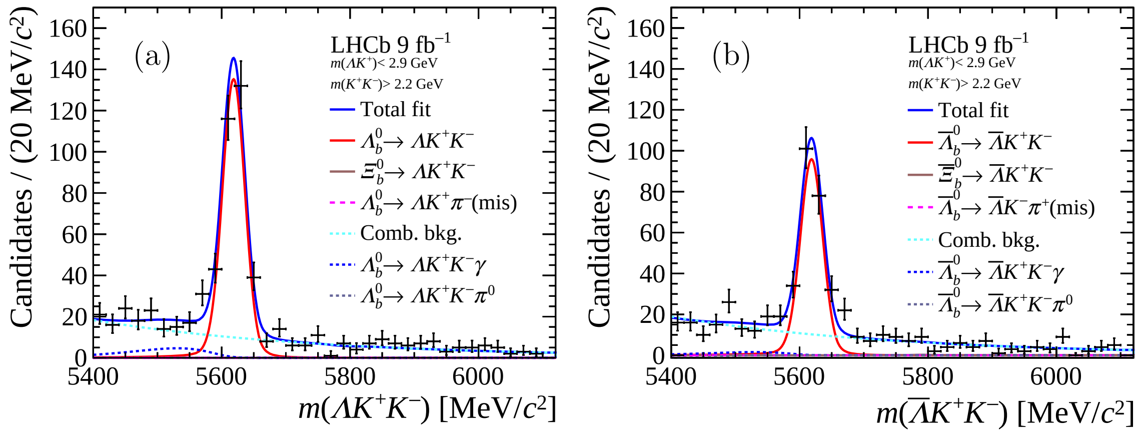

Figure 3: Mass distributions of (a) $\Lambda_b^0 \to \Lambda K^+K^-$ and (b) $\overline{\Lambda}_b^0 \to \overline{\Lambda} K^+K^-$ decays in N^* resonance-dominated regions. Also shown are the fit results.

by varying the vetoed mass regions, a new efficiency map is obtained to calculate the corresponding branching fraction and the difference is taken as a systematic uncertainty. The uncertainties on the production and experimental asymmetries are propagated to the $\Delta\mathcal{A}^{CP}$ measurements using pseudoexperiments and largely cancel in the difference of signal and control mode asymmetries. The total systematic uncertainties are obtained by summing all contributions in quadrature.

In summary, $\Lambda_b^0/\Xi_b^0 \to \Lambda h^+h'^-$ decays are studied using pp collision data collected by the LHCb experiment during LHC Runs 1–2. The $\Lambda_b^0 \to \Lambda\pi^+\pi^-$ and $\Xi_b^0 \to \Lambda K^-\pi^+$ decays are observed for the first time, and evidence is also found for the $\Xi_b^0 \to \Lambda\pi^+\pi^-$ decay. The branching-fraction measurements of $\Lambda_b^0/\Xi_b^0 \to \Lambda h^+h'^-$ decays are more precise than and supersede previous LHCb results [11]. The CP asymmetries are measured for $\Lambda_b^0 \to \Lambda h^+h'^-$ and $\Xi_b^0 \to \Lambda K^-\pi^+$ decays, with respect to the $\Lambda_b^0 \to \Lambda_c^+(\to \Lambda\pi^+)\pi^-$ decay. Evidence for CP violation is found in the $\Lambda_b^0 \to \Lambda K^+K^-$ decay for the first time, with $\Delta\mathcal{A}^{CP} = (8.3 \pm 2.8)\%$ integrated over the final-state phase space. The CP asymmetry is enhanced in the N^{*+} mass region, where it is measured to be $\Delta\mathcal{A}^{CP} = (16.5 \pm 5.1)\%$. No evidence of CP violation is found for other Λ_b^0/Ξ_b^0 decays studied. These measurements represent an important step towards establishing CP violation in baryon decays, setting the stage for future studies of quasi-two-body decays.

Acknowledgements

We express our gratitude to our colleagues in the CERN accelerator departments for the excellent performance of the LHC. We thank the technical and administrative staff at the LHCb institutes. We acknowledge support from CERN and from the national agencies: CAPES, CNPq, FAPERJ and FINEP (Brazil); MOST and NSFC (China); CNRS/IN2P3 (France); BMBF, DFG and MPG (Germany); INFN (Italy); NWO (Netherlands); MNiSW and NCN (Poland); MCID/IFA (Romania); MICIU and AEI (Spain); SNSF and SER (Switzerland); NASU (Ukraine); STFC (United Kingdom); DOE NP and NSF (USA). We acknowledge the computing resources that are provided by CERN, IN2P3 (France), KIT and DESY (Germany), INFN (Italy), SURF (Netherlands), PIC (Spain), GridPP (United

Kingdom), CSCS (Switzerland), IFIN-HH (Romania), CBPF (Brazil), and Polish WLCG (Poland). We are indebted to the communities behind the multiple open-source software packages on which we depend. Individual groups or members have received support from ARC and ARDC (Australia); Key Research Program of Frontier Sciences of CAS, CAS PIFI, CAS CCEPP, Fundamental Research Funds for the Central Universities, and Sci. & Tech. Program of Guangzhou (China); Minciencias (Colombia); EPLANET, Marie Skłodowska-Curie Actions, ERC and NextGenerationEU (European Union); A*MIDEX, ANR, IPhU and Labex P2IO, and Région Auvergne-Rhône-Alpes (France); AvH Foundation (Germany); ICSC (Italy); Severo Ochoa and María de Maeztu Units of Excellence, GVA, XuntaGal, GENCAT, InTalent-Inditex and Prog. Atracción Talento CM (Spain); SRC (Sweden); the Leverhulme Trust, the Royal Society and UKRI (United Kingdom).

End Matter

1 Summary of the fit results

Figure 4 shows the mass spectra of the $\Lambda_b^0 \to \Lambda K^+\pi^-$, $\Lambda_b^0 \to \Lambda\pi^+\pi^-$ and $\Xi_b^0 \to \Lambda K^-\pi^+$ decays, separately for baryon and antibaryon samples. Figure 5 shows the mass spectra used to obtain yields of signal channels for branching fraction calculations of (a)(b) $\Lambda_b^0(\Xi_b^0) \to \Lambda K^+K^-$, (c) $\Lambda_b^0 \to \Lambda K^+\pi^-$, (d) $\Xi_b^0 \to \Lambda K^-\pi^+$, and (e)(f) $\Lambda_b^0(\Xi_b^0) \to \Lambda K^+K^-$ decay modes. The same BDT classifier is used in selecting candidates for the Λ_b^0 and Ξ_b^0 modes, but with a different figure-of-merit (FoM) used to choose the optimal requirement. Due to the relatively smaller number of Ξ_b^0 signal yields, when determining its selection criteria the $N_{\rm S}/(\sqrt{N_{\rm B}}+2.5)$ FoM method is applied, as shown in Fig. 5 (b)(d)(f), whereas when studying the Λ_b^0 modes, the $N_{\rm S}/\sqrt{N_{\rm S}+N_{\rm B}}$ FoM method is applied, as shown in Fig. 4 and Fig. 5 (a)(c)(e). Figure 6 shows the mass spectrum of the control channel $\Lambda_b^0 \to \Lambda_c^+(\to \Lambda\pi^+)\pi^-$.

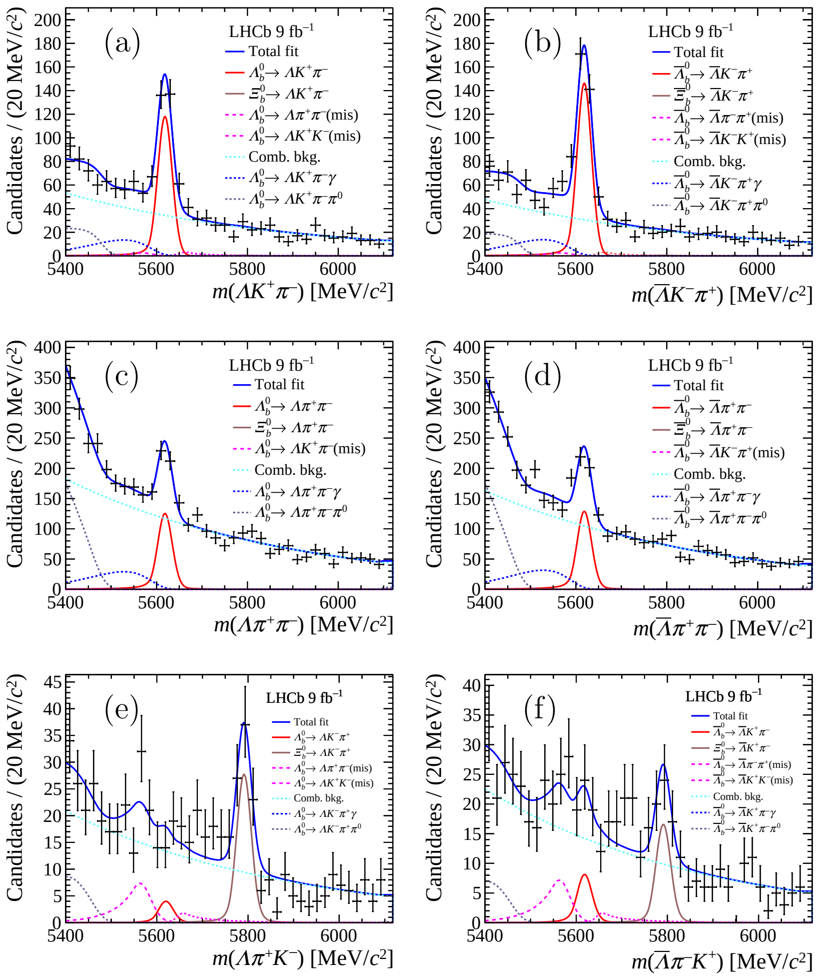

Figure 4: Distributions of $m(\Lambda h^+h^-)$ for (a) $\Lambda_b^0 \to \Lambda K^+\pi^-$, (b) $\overline{\Lambda}_b^0 \to \overline{\Lambda}K^-\pi^+$, (c) $\Lambda_b^0 \to \Lambda\pi^+\pi^-$, (d) $\overline{\Lambda}_b^0 \to \overline{\Lambda}\pi^+\pi^-$, (e) $\Xi_b^0 \to \Lambda K^-\pi^+$, and (f) $\overline{\Xi}_b^0 \to \overline{\Lambda}K^+\pi^-$ decays in data, together with the fit results. The selection criteria are optimized with the $N_{\rm S}/\sqrt{N_{\rm S}+N_{\rm B}}$ FoM for Λ_b^0 distributions and $N_{\rm S}/(\sqrt{N_{\rm B}}+2.5)$ FoM for Ξ_b^0 distributions.

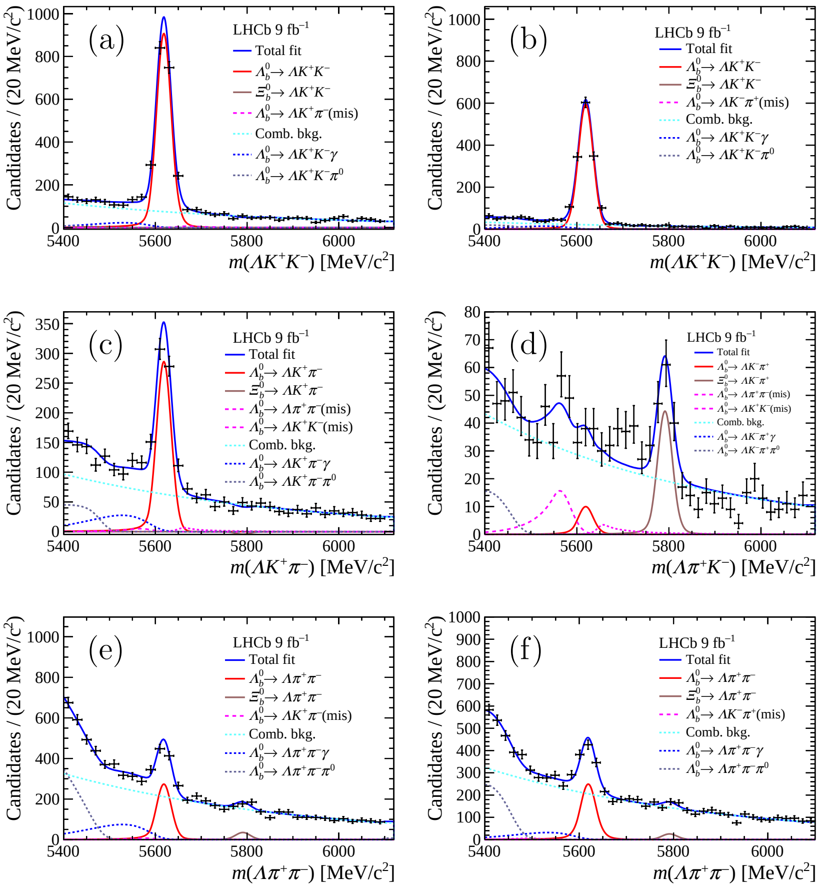

Figure 5: Distributions of $m(\Lambda h^+h^-)$ for (a)(b) $\Lambda_b^0(\Xi_b^0) \to \Lambda K^+K^-$, (c) $\Lambda_b^0 \to \Lambda K^+\pi^-$, (d) $\Xi_b^0 \to \Lambda K^-\pi^+$ and (e)(f) $\Lambda_b^0(\Xi_b^0) \to \Lambda K^+K^-$ decay modes, together with the fit results, where (a)(c)(e) are selected with the $N_S/(\sqrt{N_B+N_S})$ FoM, focusing on the Λ_b^0 studies, while (b)(d)(f) are selected with the $N_S/(\sqrt{N_B}+2.5)$ FoM for Ξ_b^0 studies.

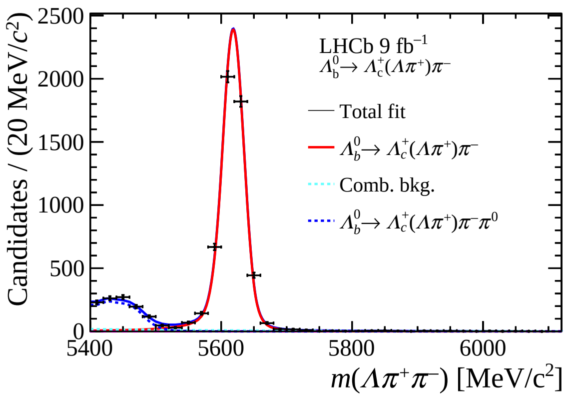

Figure 6: Mass distribution for the $\Lambda_b^0 \to \Lambda_c^+(\to \Lambda\pi^+)\pi^-$ control mode.

2 Summary tables for correction terms

Table 3 lists the production asymmetry difference ΔA_{P} and detection asymmetry difference ΔA_{exp} for each decay mode with respect to control mode.

Table 3: Production asymmetry difference ΔA_{P} and detection asymmetry difference ΔA_{exp} for each decay mode. The uncertainties from these asymmetries are propagated into the phase-space integrated $\Delta\mathcal{A}^{CP}$ as systematic uncertainties.

Channel	ΔA_{P} [%]	ΔA_{exp} [%]
$\Lambda_b^0 \to \Lambda\pi^+\pi^-$	0.1 ± 0.1	0.1 ± 0.9
$\Lambda_b^0 \to \Lambda K^+\pi^-$	0.2 ± 0.2	1.4 ± 1.0
$\Lambda_b^0 \to \Lambda K^+K^-$	-0.2 ± 0.2	0.0 ± 0.9
$\Xi_b^0 \to \Lambda K^-\pi^+$	-5.2 ± 4.0	0.3 ± 1.6

3 Summary figures and tables for adaptive binnning scheme

Figure 7 shows the two dimensional mass distributions for (a) $\Lambda_b^0 \to \Lambda K^+K^-$, (b) $\Lambda_b^0 \to \Lambda K^+\pi^-$, and (c) $\Lambda_b^0 \to \Lambda\pi^+\pi^-$, along with the bin boundaries used for the adaptive binning scheme. Table 4 lists the bin definitions used for each decay mode in the adaptive binning scheme and the per-bin CP asymmetry measurements.

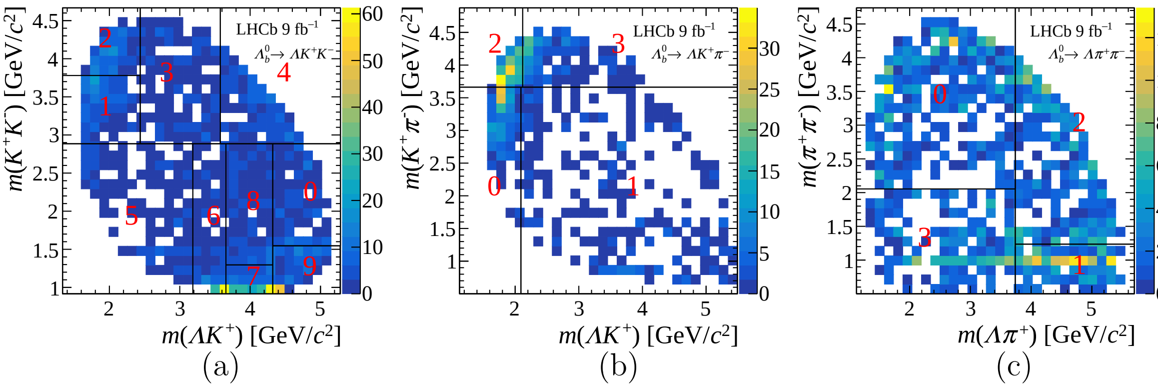

Figure 7: Two dimensional mass distributions for (a) $\Lambda_b^0 \to \Lambda K^+K^-$, (b) $\Lambda_b^0 \to \Lambda K^+\pi^-$, and (c) $\Lambda_b^0 \to \Lambda\pi^+\pi^-$ decays in data. The boundaries for the adaptive binning scheme are drawn as solid lines.

Table 4: Boundaries of the adaptive binning scheme and the $\Delta\mathcal{A}^{CP}$ measurements from each bin, the first uncertainty is statistical and the second is systematic. The variables of the x and y axes and the bin numbers in the table are those presented in Fig. 7. The reported ranges are expressed in GeV/c^2.

Channel	bin number	x-low	x-high	y-low	y-high	$\Delta\mathcal{A}^{CP}$
$\Lambda_b^0 \to \Lambda\pi^+\pi^-$	0	1.13	3.74	2.05	4.74	$-0.483 \pm 0.200 \pm 0.043$
	1	3.74	5.50	0.50	1.24	$0.147 \pm 0.092 \pm 0.026$
	2	3.74	5.50	1.24	4.74	$0.058 \pm 0.114 \pm 0.028$
	3	1.13	3.74	0.50	2.05	$0.067 \pm 0.111 \pm 0.028$
$\Lambda_b^0 \to \Lambda K^+\pi^-$	0	1.13	2.09	0.50	3.66	$-0.153 \pm 0.079 \pm 0.027$
	1	2.09	5.49	0.50	3.66	$-0.284 \pm 0.188 \pm 0.041$
	2	1.13	2.12	3.66	4.87	$-0.006 \pm 0.062 \pm 0.028$
	3	2.12	5.49	3.66	4.87	$-0.264 \pm 0.125 \pm 0.030$
$\Lambda_b^0 \to \Lambda K^+K^-$	0	4.32	5.08	1.55	2.88	$0.017 \pm 0.092 \pm 0.025$
	1	1.33	2.44	2.88	3.78	$0.188 \pm 0.075 \pm 0.023$
	2	1.33	2.44	3.78	4.67	$0.062 \pm 0.077 \pm 0.022$
	3	2.44	3.58	2.88	4.67	$0.064 \pm 0.093 \pm 0.024$
	4	3.58	5.08	2.88	4.67	$0.088 \pm 0.077 \pm 0.022$
	5	1.33	3.19	0.92	2.88	$0.061 \pm 0.089 \pm 0.024$
	6	3.19	3.66	0.92	2.88	$0.066 \pm 0.088 \pm 0.024$
	7	3.66	4.32	0.92	1.30	$0.168 \pm 0.070 \pm 0.021$
	8	3.66	4.32	1.30	2.88	$-0.002 \pm 0.080 \pm 0.023$
	9	4.32	5.08	0.92	1.55	$0.025 \pm 0.074 \pm 0.022$

References

[1] Heavy Flavor Averaging Group, Y. Amhis *et al.*, *Averages of b-hadron, c-hadron, and τ-lepton properties as of 2021*, Phys. Rev. **D107** (2023) 052008, arXiv:2206.07501, updated results and plots available at https://hflav.web.cern.ch.

[2] A. Riotto and M. Trodden, *Recent progress in baryogenesis*, Ann. Rev. Nucl. Part. Sci. **49** (1999) 35, arXiv:hep-ph/9901362.

[3] BESIII collaboration, M. Ablikim *et al.*, *Precise measurements of decay parameters and CP asymmetry with entangled $\Lambda - \bar{\Lambda}$ pairs*, Phys. Rev. Lett. **129** (2022) 131801, arXiv:2204.11058.

[4] LHCb collaboration, R. Aaij *et al.*, *Searches for Λ_b^0 and Ξ_b^0 decays to $K_S^0 p\pi^-$ and $K_S^0 pK^-$ final states with first observation of the $\Lambda_b^0 \to K_S^0 p\pi^-$ decay*, JHEP **04** (2014) 087, arXiv:1402.0770.

[5] LHCb collaboration, R. Aaij *et al.*, *Observation of the $\Lambda_b^0 \to J/\psi p\pi^-$ decay*, JHEP **07** (2014) 103, arXiv:1406.0755.

[6] LHCb collaboration, R. Aaij *et al.*, *Measurement of matter-antimatter differences in beauty baryon decays*, Nature Physics **13** (2017) 391, arXiv:1609.05216.

[7] LHCb collaboration, R. Aaij *et al.*, *Search for CP violation using triple product asymmetries in $\Lambda_b^0 \to pK^-\pi^+\pi^-$, $\Lambda_b^0 \to pK^-K^+K^-$, and $\Xi_b^0 \to pK^-K^-\pi^+$ decays*, JHEP **08** (2018) 039, arXiv:1805.03941.

[8] LHCb collaboration, R. Aaij *et al.*, *Measurement of CP asymmetries in charmless four-body Λ_b^0 and Ξ_b^0 decays*, Eur. Phys. J. **C79** (2019) 745, arXiv:1903.06792.

[9] LHCb collaboration, R. Aaij *et al.*, *Search for CP violation and observation of P violation in $\Lambda_b^0 \to p\pi^-\pi^+\pi^-$ decays*, Phys. Rev. **D102** (2020) 051101, arXiv:1912.10741.

[10] LHCb collaboration, R. Aaij *et al.*, *Observation of the suppressed $\Lambda_b^0 \to DpK^-$ decay with $D \to K^+\pi^-$ and measurement of its CP asymmetry*, Phys. Rev. **D104** (2021) 112008, arXiv:2109.02621.

[11] LHCb collaboration, R. Aaij *et al.*, *Observations of $\Lambda_b^0 \to \Lambda K^+\pi^-$ and $\Lambda_b^0 \to \Lambda K^+K^-$ decays and searches for other Λ_b^0 and Ξ_b^0 decays to Λh^+h^- final states*, JHEP **05** (2016) 081, arXiv:1603.00413.

[12] LHCb collaboration, R. Aaij *et al.*, *Observation of the decay $\Lambda_b^0 \to pK^-\mu^+\mu^-$ and search for CP violation*, JHEP **06** (2017) 108, arXiv:1703.00256.

[13] LHCb collaboration, R. Aaij *et al.*, *Search for CP violation in $\Lambda_b^0 \to pK^-$ and $\Lambda_b^0 \to p\pi^-$ decays*, Phys. Lett. **B784** (2018) 101, arXiv:1807.06544.

[14] LHCb collaboration, R. Aaij *et al.*, *Search for CP violation in $\Xi_b^- \to pK^-K^-$decays*, Phys. Rev. **D104** (2021) 052010, arXiv:2104.15074.

[15] LHCb collaboration, R. Aaij *et al.*, *Measurement of the photon polarization in $\Lambda_b^0 \to \Lambda\gamma$ decays*, Phys. Rev. **D105** (2022) 051104, arXiv:2111.10194.

[16] LHCb collaboration, R. Aaij *et al.*, *Observation of the $\Lambda_b^0 \to \Lambda\phi$ decay*, Phys. Lett. **B759** (2016) 282, arXiv:1603.02870.

[17] LHCb collaboration, R. Aaij *et al.*, *Search for CP violation in $\Lambda_c^+ \to pK^-K^+$ and $\Lambda_c^+ \to p\pi^-\pi^+$ decays*, JHEP **03** (2018) 182, arXiv:1712.07051.

[18] LHCb collaboration, R. Aaij *et al.*, *Search for CP violation in $\Xi_c^+ \to pK^-\pi^+$ decays with model-independent techniques*, Eur. Phys. J. **C80** (2020) 986, arXiv:2006.03145.

[19] LHCb collaboration, R. Aaij *et al.*, *Direct CP violation in charmless three-body decays of $B^\pm$ mesons*, Phys. Rev. **D108** (2023) 012008, arXiv:2206.07622.

[20] LHCb collaboration, R. Aaij *et al.*, *Amplitude analysis of $B^\pm \to \pi^\pm K^+K^-$ decays*, Phys. Rev. Lett. **123** (2019) 231802, arXiv:1905.09244.

[21] LHCb collaboration, R. Aaij *et al.*, *Measurement of CP violation in the three-body phase space of charmless $B^\pm$ decays*, Phys. Rev. **D90** (2014) 112004, arXiv:1408.5373.

[22] C. Q. Geng, Y. K. Hsiao, Y.-H. Lin, and Y. Yu, *Study of $\Lambda_b^0 \to \Lambda(\phi, \eta^{(\prime)})$ and $\Lambda_b^0 \to \Lambda K^+K^-$ decays*, Eur. Phys. J. **C76** (2016) 399, arXiv:1603.06682.

[23] S. Arunagiri and C. Q. Geng, *T violating triple product asymmetries in $\Lambda_b^0 \to \Lambda\pi^+\pi^-$ decay*, Phys. Rev. **D69** (2004) 017901, arXiv:hep-ph/0307307.

[24] X.-H. Guo and A. W. Thomas, *Direct CP violation in $\Lambda_b^0 \to n_\Lambda\pi^+\pi^-$ decays via $\rho - \omega$ mixing*, Phys. Rev. **D58** (1998) 096013, arXiv:hep-ph/9805332.

[25] J. Zhu, Z.-T. Wei, and H.-W. Ke, *Semileptonic and nonleptonic weak decays of Λ_b^0*, Phys. Rev. **D99** (2019) 054020.

[26] Z. Rui, J.-M. Li, and C.-Q. Zhang, *Estimates of exchange topological contributions and CP-violating observables in $\Lambda_b^0 \to \Lambda\phi$ decay*, Phys. Rev. **D107** (2023) 053009, arXiv:2210.15357.

[27] Y. K. Hsiao, Y. Yao, and C. Q. Geng, *Charmless two-body antitriplet b-baryon decays*, Phys. Rev. **D95** (2017) 093001.

[28] J.-P. Wang and F.-S. Yu, *CP violation of baryon decays with $N\pi$ rescatterings*, Chinese Physics **C48** (2024) 101001.

[29] LHCb collaboration, A. A. Alves Jr. *et al.*, *The LHCb detector at the LHC*, JINST **3** (2008) S08005.

[30] LHCb collaboration, R. Aaij *et al.*, *LHCb detector performance*, Int. J. Mod. Phys. **A30** (2015) 1530022, arXiv:1412.6352.

[31] R. Arink *et al.*, *Performance of the LHCb Outer Tracker*, JINST **9** (2014) P01002, arXiv:1311.3893.

[32] P. d'Argent *et al.*, *Improved performance of the LHCb Outer Tracker in LHC Run 2*, JINST **12** (2017) P11016, arXiv:1708.00819.

[33] M. Adinolfi *et al.*, *Performance of the LHCb RICH detector at the LHC*, Eur. Phys. J. **C73** (2013) 2431, arXiv:1211.6759.

[34] L. Anderlini *et al.*, *The PIDCalib package*, LHCb-PUB-2016-021, 2016.

[35] R. Aaij *et al.*, *Design and performance of the LHCb trigger and full real-time reconstruction in Run 2 of the LHC*, JINST **14** (2019) P04013, arXiv:1812.10790.

[36] R. Aaij *et al.*, *The LHCb trigger and its performance in 2011*, JINST **8** (2013) P04022, arXiv:1211.3055.

[37] T. Sjöstrand, S. Mrenna, and P. Skands, *A brief introduction to PYTHIA 8.1*, Comput. Phys. Commun. **178** (2008) 852, arXiv:0710.3820; T. Sjöstrand, S. Mrenna, and P. Skands, *PYTHIA 6.4 physics and manual*, JHEP **05** (2006) 026, arXiv:hep-ph/0603175.

[38] D. J. Lange, *The EvtGen particle decay simulation package*, Nucl. Instrum. Meth. **A462** (2001) 152.

[39] P. Golonka and Z. Was, *PHOTOS Monte Carlo: A precision tool for QED corrections in Z and W decays*, Eur. Phys. J. **C45** (2006) 97, arXiv:hep-ph/0506026.

[40] Geant4 collaboration, J. Allison *et al.*, *Geant4 developments and applications*, IEEE Trans. Nucl. Sci. **53** (2006) 270; Geant4 collaboration, S. Agostinelli *et al.*, *Geant4: A simulation toolkit*, Nucl. Instrum. Meth. **A506** (2003) 250.

[41] M. Clemencic *et al.*, *The LHCb simulation application, Gauss: Design, evolution and experience*, J. Phys. Conf. Ser. **331** (2011) 032023.

[42] L. Breiman, J. H. Friedman, R. A. Olshen, and C. J. Stone, *Classification and regression trees*, Wadsworth international group, Belmont, California, USA, 1984.

[43] H. Voss, A. Hoecker, J. Stelzer, and F. Tegenfeldt, *TMVA - Toolkit for Multivariate Data Analysis with ROOT*, PoS **ACAT** (2007) 040.

[44] Particle Data Group, S. Navas *et al.*, *Review of particle physics*, Phys. Rev. **D110** (2024) 030001.

[45] T. Skwarnicki, *A study of the radiative cascade transitions between the Upsilon-prime and Upsilon resonances*, PhD thesis, Institute of Nuclear Physics, Krakow, 1986, DESY-F31-86-02.

[46] ARGUS collaboration, H. Albrecht *et al.*, *Search for hadronic $b \to u$ decays*, Phys. Lett. **B241** (1990) 278.

[47] S. S. Wilks, *The large-sample distribution of the likelihood ratio for testing composite hypotheses*, Ann. Math. Stat. **9** (1938) 60.

[48] LHCb collaboration, R. Aaij *et al.*, *Study of the kinematic dependences of Λ_b^0 production in pp collisions and a measurement of the $\Lambda_b^0 \to \Lambda_c^+ \pi^-$ branching fraction*, JHEP **08** (2014) 143, arXiv:1405.6842.

[49] LHCb collaboration, R. Aaij *et al.*, *Measurement of the mass and production rate of Ξ_b^- baryons*, Phys. Rev. **D99** (2019) 052006, arXiv:1901.07075.

[50] LHCb collaboration, R. Aaij *et al.*, *Measurement of forward J/ψ production cross-sections in pp collisions at $\sqrt{s}=13$ TeV*, JHEP **10** (2015) 172, Erratum ibid. **05** (2017) 063, arXiv:1509.00771.

[51] BESIII collaboration, M. Ablikim *et al.*, *Measurements of absolute hadronic branching fractions of Λ_c^+ baryon*, Phys. Rev. Lett. **116** (2016) 052001, arXiv:1511.08380.

[52] LHCb collaboration, R. Aaij *et al.*, *Search for the rare hadronic decay $B_s^0 \to p\overline{p}$*, Phys. Rev. **D108** (2023) 012007, arXiv:2206.06673.

[53] LHCb collaboration, R. Aaij *et al.*, *Measurement of CP asymmetry in $D^0 \to K^-K^+$ and $D^0 \to \pi^-\pi^+$ decays*, JHEP **07** (2014) 041, arXiv:1405.2797.

[54] LHCb collaboration, R. Aaij *et al.*, *Search for prompt production of pentaquarks in open charm hadron final states*, Phys. Rev. **D110** (2024) 032001, arXiv:2404.07131.

[55] M. Pivk and F. R. Le Diberder, *sPlot: A statistical tool to unfold data distributions*, Nucl. Instrum. Meth. **A555** (2005) 356, arXiv:physics/0402083.

[56] D. Martínez Santos and F. Dupertuis, *Mass distributions marginalized over per-event errors*, Nucl. Instrum. Meth. **A764** (2014) 150, arXiv:1312.5000.

LHCb collaboration

R. Aaij[38], A.S.W. Abdelmotteleb[57], C. Abellan Beteta[51], F. Abudinén[57], T. Ackernley[61], A. A. Adefisoye[69], B. Adeva[47], M. Adinolfi[55], P. Adlarson[82], C. Agapopoulou[14], C.A. Aidala[83], Z. Ajaltouni[11], S. Akar[66], K. Akiba[38], P. Albicocco[28], J. Albrecht[19], F. Alessio[49], M. Alexander[60], Z. Aliouche[63], P. Alvarez Cartelle[56], R. Amalric[16], S. Amato[3], J.L. Amey[55], Y. Amhis[14], L. An[6], L. Anderlini[27], M. Andersson[51], A. Andreianov[44], P. Andreola[51], M. Andreotti[26], D. Andreou[69], A. Anelli[31,n], D. Ao[7], F. Archilli[37,t], M. Argenton[26], S. Arguedas Cuendis[9,49], A. Artamonov[44], M. Artuso[69], E. Aslanides[13], R. Ataíde Da Silva[50], M. Atzeni[65], B. Audurier[12], D. Bacher[64], I. Bachiller Perea[10], S. Bachmann[22], M. Bachmayer[50], J.J. Back[57], P. Baladron Rodriguez[47], V. Balagura[15], A. Balboni[26], W. Baldini[26], L. Balzani[19], H. Bao[7], J. Baptista de Souza Leite[61], C. Barbero Pretel[47,12], M. Barbetti[27], I. R. Barbosa[70], R.J. Barlow[63], M. Barnyakov[25], S. Barsuk[14], W. Barter[59], M. Bartolini[56], J. Bartz[69], J.M. Basels[17], S. Bashir[40], G. Bassi[35,q], B. Batsukh[5], P. B. Battista[14], A. Bay[50], A. Beck[57], M. Becker[19], F. Bedeschi[35], I.B. Bediaga[2], N. A. Behling[19], S. Belin[47], K. Belous[44], I. Belov[29], I. Belyaev[36], G. Benane[13], G. Bencivenni[28], E. Ben-Haim[16], A. Berezhnoy[44], R. Bernet[51], S. Bernet Andres[45], A. Bertolin[33], C. Betancourt[51], F. Betti[59], J. Bex[56], Ia. Bezshyiko[51], J. Bhom[41], M.S. Bieker[19], N.V. Biesuz[26], P. Billoir[16], A. Biolchini[38], M. Birch[62], F.C.R. Bishop[10], A. Bitadze[63], A. Bizzeti, T. Blake[57], F. Blanc[50], J.E. Blank[19], S. Blusk[69], V. Bocharnikov[44], J.A. Boelhauve[19], O. Boente Garcia[15], T. Boettcher[66], A. Bohare[59], A. Boldyrev[44], C.S. Bolognani[79], R. Bolzonella[26,k], R. B. Bonacci[1], N. Bondar[44], A. Bordelius[49], F. Borgato[33,o], S. Borghi[63], M. Borsato[31,n], J.T. Borsuk[41], S.A. Bouchiba[50], M. Bovill[64], T.J.V. Bowcock[61], A. Boyer[49], C. Bozzi[26], A. Brea Rodriguez[50], N. Breer[19], J. Brodzicka[41], A. Brossa Gonzalo[47,†], J. Brown[61], D. Brundu[32], E. Buchanan[59], A. Buonaura[51], L. Buonincontri[33,o], A.T. Burke[63], C. Burr[49], J.S. Butter[56], J. Buytaert[49], W. Byczynski[49], S. Cadeddu[32], H. Cai[74], A. C. Caillet[16], R. Calabrese[26,k], S. Calderon Ramirez[9], L. Calefice[46], S. Cali[28], M. Calvi[31,n], M. Calvo Gomez[45], P. Camargo Magalhaes[2,x], J. I. Cambon Bouzas[47], P. Campana[28], D.H. Campora Perez[79], A.F. Campoverde Quezada[7], S. Capelli[31], L. Capriotti[26], R. Caravaca-Mora[9], A. Carbone[25,i], L. Carcedo Salgado[47], R. Cardinale[29,l], A. Cardini[32], P. Carniti[31,n], L. Carus[22], A. Casais Vidal[65], R. Caspary[22], G. Casse[61], M. Cattaneo[49], G. Cavallero[26,49], V. Cavallini[26,k], S. Celani[22], D. Cervenkov[64], S. Cesare[30,m], A.J. Chadwick[61], I. Chahrour[83], M. Charles[16], Ph. Charpentier[49], E. Chatzianagnostou[38], M. Chefdeville[10], C. Chen[13], S. Chen[5], Z. Chen[7], A. Chernov[41], S. Chernyshenko[53], X. Chiotopoulos[79], V. Chobanova[81], S. Cholak[50], M. Chrzaszcz[41], A. Chubykin[44], V. Chulikov[28], P. Ciambrone[28], X. Cid Vidal[47], G. Ciezarek[49], P. Cifra[49], P.E.L. Clarke[59], M. Clemencic[49], H.V. Cliff[56], J. Closier[49], C. Cocha Toapaxi[22], V. Coco[49], J. Cogan[13], E. Cogneras[11], L. Cojocariu[43], S. Collaviti[50], P. Collins[49], T. Colombo[49], M. C. Colonna[19], A. Comerma-Montells[46], L. Congedo[24], A. Contu[32], N. Cooke[60], I. Corredoira [47], A. Correia[16], G. Corti[49], J.J. Cottee Meldrum[55], B. Couturier[49], D.C. Craik[51], M. Cruz Torres[2,f], E. Curras Rivera[50], R. Currie[59], C.L. Da Silva[68], S. Dadabaev[44], L. Dai[71], X. Dai[6], E. Dall'Occo[49], J. Dalseno[47], C. D'Ambrosio[49], J. Daniel[11], A. Danilina[44], P. d'Argent[24], G. Darze[3], A. Davidson[57], J.E. Davies[63], A. Davis[63], O. De Aguiar Francisco[63], C. De Angelis[32,j], F. De Benedetti[49], J. de Boer[38], K. De Bruyn[78], S. De Capua[63], M. De Cian[22],

U. De Freitas Carneiro Da Graca[2,a], E. De Lucia[28], J.M. De Miranda[2], L. De Paula[3], M. De Serio[24,g], P. De Simone[28], F. De Vellis[19], J.A. de Vries[79], F. Debernardis[24], D. Decamp[10], V. Dedu[13], S. Dekkers[1], L. Del Buono[16], B. Delaney[65], H.-P. Dembinski[19], J. Deng[8], V. Denysenko[51], O. Deschamps[11], F. Dettori[32,j], B. Dey[77], P. Di Nezza[28], I. Diachkov[44], S. Didenko[44], S. Ding[69], L. Dittmann[22], V. Dobishuk[53], A. D. Docheva[60], C. Dong[4,b], A.M. Donohoe[23], F. Dordei[32], A.C. dos Reis[2], A. D. Dowling[69], W. Duan[72], P. Duda[80], M.W. Dudek[41], L. Dufour[49], V. Duk[34], P. Durante[49], M. M. Duras[80], J.M. Durham[68], O. D. Durmus[77], A. Dziurda[41], A. Dzyuba[44], S. Easo[58], E. Eckstein[18], U. Egede[1], A. Egorychev[44], V. Egorychev[44], S. Eisenhardt[59], E. Ejopu[63], L. Eklund[82], M. Elashri[66], J. Ellbracht[19], S. Ely[62], A. Ene[43], J. Eschle[69], S. Esen[22], T. Evans[63], F. Fabiano[32,j], L.N. Falcao[2], Y. Fan[7], B. Fang[7], L. Fantini[34,p,49], M. Faria[50], K. Farmer[59], D. Fazzini[31,n], L. Felkowski[80], M. Feng[5,7], M. Feo[19], A. Fernandez Casani[48], M. Fernandez Gomez[47], A.D. Fernez[67], F. Ferrari[25], F. Ferreira Rodrigues[3], M. Ferrillo[51], M. Ferro-Luzzi[49], S. Filippov[44], R.A. Fini[24], M. Fiorini[26,k], M. Firlej[40], K.L. Fischer[64], D.S. Fitzgerald[83], C. Fitzpatrick[63], T. Fiutowski[40], F. Fleuret[15], M. Fontana[25], L. F. Foreman[63], R. Forty[49], D. Foulds-Holt[56], V. Franco Lima[3], M. Franco Sevilla[67], M. Frank[49], E. Franzoso[26,k], G. Frau[63], C. Frei[49], D.A. Friday[63], J. Fu[7], Q. Fuehring[19,56], Y. Fujii[1], T. Fulghesu[16], E. Gabriel[38], G. Galati[24], M.D. Galati[38], A. Gallas Torreira[47], D. Galli[25,i], S. Gambetta[59], M. Gandelman[3], P. Gandini[30], B. Ganie[63], H. Gao[7], R. Gao[64], T.Q. Gao[56], Y. Gao[8], Y. Gao[6], Y. Gao[8], L.M. Garcia Martin[50], P. Garcia Moreno[46], J. García Pardiñas[49], P. Gardner[67], K. G. Garg[8], L. Garrido[46], C. Gaspar[49], R.E. Geertsema[38], L.L. Gerken[19], E. Gersabeck[63], M. Gersabeck[20], T. Gershon[57], S. G. Ghizzo[29,l], Z. Ghorbanimoghaddam[55], L. Giambastiani[33,o], F. I. Giasemis[16,e], V. Gibson[56], H.K. Giemza[42], A.L. Gilman[64], M. Giovannetti[28], A. Gioventù[46], L. Girardey[63], P. Gironella Gironell[46], C. Giugliano[26,k], M.A. Giza[41], E.L. Gkougkousis[62], F.C. Glaser[14,22], V.V. Gligorov[16,49], C. Göbel[70], E. Golobardes[45], D. Golubkov[44], A. Golutvin[62,44,49], S. Gomez Fernandez[46], W. Gomulka[40], F. Goncalves Abrantes[64], M. Goncerz[41], G. Gong[4,b], J. A. Gooding[19], I.V. Gorelov[44], C. Gotti[31], J.P. Grabowski[18], L.A. Granado Cardoso[49], E. Graugés[46], E. Graverini[50,r], L. Grazette[57], G. Graziani, A. T. Grecu[43], L.M. Greeven[38], N.A. Grieser[66], L. Grillo[60], S. Gromov[44], C. Gu[15], M. Guarise[26], L. Guerry[11], M. Guittiere[14], V. Guliaeva[44], P. A. Günther[22], A.-K. Guseinov[50], E. Gushchin[44], Y. Guz[6,44,49], T. Gys[49], K. Habermann[18], T. Hadavizadeh[1], C. Hadjivasiliou[67], G. Haefeli[50], C. Haen[49], M. Hajheidari[49], G. Hallett[57], M.M. Halvorsen[49], P.M. Hamilton[67], J. Hammerich[61], Q. Han[8], X. Han[22,49], S. Hansmann-Menzemer[22], L. Hao[7], N. Harnew[64], T. H. Harris[1], M. Hartmann[14], S. Hashmi[40], J. He[7,c], F. Hemmer[49], C. Henderson[66], R.D.L. Henderson[1,57], A.M. Hennequin[49], K. Hennessy[61], L. Henry[50], J. Herd[62], P. Herrero Gascon[22], J. Heuel[17], A. Hicheur[3], G. Hijano Mendizabal[51], J. Horswill[63], R. Hou[8], Y. Hou[11], N. Howarth[61], J. Hu[72], W. Hu[6], X. Hu[4,b], W. Huang[7], W. Hulsbergen[38], R.J. Hunter[57], M. Hushchyn[44], D. Hutchcroft[61], M. Idzik[40], D. Ilin[44], P. Ilten[66], A. Inglessi[44], A. Iniukhin[44], A. Ishteev[44], K. Ivshin[44], R. Jacobsson[49], H. Jage[17], S.J. Jaimes Elles[75,49,48], S. Jakobsen[49], E. Jans[38], B.K. Jashal[48], A. Jawahery[67,49], V. Jevtic[19], E. Jiang[67], X. Jiang[5,7], Y. Jiang[7], Y. J. Jiang[6], M. John[64], A. John Rubesh Rajan[23], D. Johnson[54], C.R. Jones[56], T.P. Jones[57], S. Joshi[42], B. Jost[49], J. Juan Castella[56], N. Jurik[49], I. Juszczak[41], D. Kaminaris[50], S. Kandybei[52], M. Kane[59], Y. Kang[4,b], C. Kar[11], M. Karacson[49],

D. Karpenkov[44], A. Kauniskangas[50], J.W. Kautz[66], M.K. Kazanecki[41], F. Keizer[49], M. Kenzie[56], T. Ketel[38], B. Khanji[69], A. Kharisova[44], S. Kholodenko[35,49], G. Khreich[14], T. Kirn[17], V.S. Kirsebom[31,n], O. Kitouni[65], S. Klaver[39], N. Kleijne[35,q], K. Klimaszewski[42], M.R. Kmiec[42], S. Koliiev[53], L. Kolk[19], A. Konoplyannikov[44], P. Kopciewicz[40,49], P. Koppenburg[38], M. Korolev[44], I. Kostiuk[38], O. Kot[53], S. Kotriakhova, A. Kozachuk[44], P. Kravchenko[44], L. Kravchuk[44], M. Kreps[57], P. Krokovny[44], W. Krupa[69], W. Krzemien[42], O.K. Kshyvanskyi[53], S. Kubis[80], M. Kucharczyk[41], V. Kudryavtsev[44], E. Kulikova[44], A. Kupsc[82], B. K. Kutsenko[13], D. Lacarrere[49], P. Laguarta Gonzalez[46], A. Lai[32], A. Lampis[32], D. Lancierini[56], C. Landesa Gomez[47], J.J. Lane[1], R. Lane[55], G. Lanfranchi[28], C. Langenbruch[22], J. Langer[19], O. Lantwin[44], T. Latham[57], F. Lazzari[35,r], C. Lazzeroni[54], R. Le Gac[13], H. Lee[61], R. Lefèvre[11], A. Leflat[44], S. Legotin[44], M. Lehuraux[57], E. Lemos Cid[49], O. Leroy[13], T. Lesiak[41], E. Lesser[49], B. Leverington[22], A. Li[4,b], C. Li[13], H. Li[72], K. Li[8], L. Li[63], M. Li[8], P. Li[7], P.-R. Li[73], Q. Li[5,7], S. Li[8], T. Li[5,d], T. Li[72], Y. Li[8], Y. Li[5], Z. Lian[4,b], X. Liang[69], S. Libralon[48], C. Lin[7], T. Lin[58], R. Lindner[49], H. Linton[62], V. Lisovskyi[50], R. Litvinov[32,49], F. L. Liu[1], G. Liu[72], K. Liu[73], S. Liu[5,7], W. Liu[8], Y. Liu[59], Y. Liu[73], Y. L. Liu[62], A. Lobo Salvia[46], A. Loi[32], T. Long[56], J.H. Lopes[3], A. Lopez Huertas[46], S. López Soliño[47], Q. Lu[15], C. Lucarelli[27], D. Lucchesi[33,o], M. Lucio Martinez[79], V. Lukashenko[38,53], Y. Luo[6], A. Lupato[33,h], E. Luppi[26,k], K. Lynch[23], X.-R. Lyu[7], G. M. Ma[4,b], S. Maccolini[19], F. Machefert[14], F. Maciuc[43], B. Mack[69], I. Mackay[64], L. M. Mackey[69], L.R. Madhan Mohan[56], M. J. Madurai[54], A. Maevskiy[44], D. Magdalinski[38], D. Maisuzenko[44], M.W. Majewski[40], J.J. Malczewski[41], S. Malde[64], L. Malentacca[49], A. Malinin[44], T. Maltsev[44], G. Manca[32,j], G. Mancinelli[13], C. Mancuso[30,14,m], R. Manera Escalero[46], F. M. Manganella[37], D. Manuzzi[25], D. Marangotto[30,m], J.F. Marchand[10], R. Marchevski[50], U. Marconi[25], E. Mariani[16], S. Mariani[49], C. Marin Benito[46,49], J. Marks[22], A.M. Marshall[55], L. Martel[64], G. Martelli[34,p], G. Martellotti[36], L. Martinazzoli[49], M. Martinelli[31,n], D. Martinez Gomez[78], D. Martinez Santos[81], F. Martinez Vidal[48], A. Martorell i Granollers[45], A. Massafferri[2], R. Matev[49], A. Mathad[49], V. Matiunin[44], C. Matteuzzi[69], K.R. Mattioli[15], A. Mauri[62], E. Maurice[15], J. Mauricio[46], P. Mayencourt[50], J. Mazorra de Cos[48], M. Mazurek[42], M. McCann[62], L. Mcconnell[23], T.H. McGrath[63], N.T. McHugh[60], A. McNab[63], R. McNulty[23], B. Meadows[66], G. Meier[19], D. Melnychuk[42], F. M. Meng[4,b], M. Merk[38,79], A. Merli[50], L. Meyer Garcia[67], D. Miao[5,7], H. Miao[7], M. Mikhasenko[76], D.A. Milanes[75], A. Minotti[31,n], E. Minucci[28], T. Miralles[11], B. Mitreska[19], D.S. Mitzel[19], A. Modak[58], R.A. Mohammed[64], R.D. Moise[17], S. Mokhnenko[44], E. F. Molina Cardenas[83], T. Mombächer[49], M. Monk[57,1], S. Monteil[11], A. Morcillo Gomez[47], G. Morello[28], M.J. Morello[35,q], M.P. Morgenthaler[22], J. Moron[40], W. Morren[38], A.B. Morris[49], A.G. Morris[13], R. Mountain[69], H. Mu[4,b], Z. M. Mu[6], E. Muhammad[57], F. Muheim[59], M. Mulder[78], K. Müller[51], F. Muñoz-Rojas[9], R. Murta[62], P. Naik[61], T. Nakada[50], R. Nandakumar[58], T. Nanut[49], I. Nasteva[3], M. Needham[59], N. Neri[30,m], S. Neubert[18], N. Neufeld[49], P. Neustroev[44], J. Nicolini[19,14], D. Nicotra[79], E.M. Niel[49], N. Nikitin[44], P. Nogarolli[3], P. Nogga[18], C. Normand[55], J. Novoa Fernandez[47], G. Nowak[66], C. Nunez[83], H. N. Nur[60], A. Oblakowska-Mucha[40], V. Obraztsov[44], T. Oeser[17], S. Okamura[26,k], A. Okhotnikov[44], O. Okhrimenko[53], R. Oldeman[32,j], F. Oliva[59], M. Olocco[19], C.J.G. Onderwater[79], R.H. O'Neil[59], D. Osthues[19], J.M. Otalora Goicochea[3], P. Owen[51], A. Oyanguren[48], O. Ozcelik[59], F. Paciolla[35,u],

A. Padee[42], K.O. Padeken[18], B. Pagare[57], P.R. Pais[22], T. Pajero[49], A. Palano[24], M. Palutan[28], X. Pan[4,b], G. Panshin[44], L. Paolucci[57], A. Papanestis[58,49], M. Pappagallo[24,g], L.L. Pappalardo[26,k], C. Pappenheimer[66], C. Parkes[63], D. Parmar[76], B. Passalacqua[26,k], G. Passaleva[27], D. Passaro[35,q], A. Pastore[24], M. Patel[62], J. Patoc[64], C. Patrignani[25,i], A. Paul[69], C.J. Pawley[79], A. Pellegrino[38], J. Peng[5,7], M. Pepe Altarelli[28], S. Perazzini[25], D. Pereima[44], H. Pereira Da Costa[68], A. Pereiro Castro[47], P. Perret[11], A. Perrevoort[78], A. Perro[49], M.J. Peters[66], K. Petridis[55], A. Petrolini[29,l], J. P. Pfaller[66], H. Pham[69], L. Pica[35,q], M. Piccini[34], L. Piccolo[32], B. Pietrzyk[10], G. Pietrzyk[14], D. Pinci[36], F. Pisani[49], M. Pizzichemi[31,n,49], V. Placinta[43], M. Plo Casasus[47], T. Poeschl[49], F. Polci[16,49], M. Poli Lener[28], A. Poluektov[13], N. Polukhina[44], I. Polyakov[44], E. Polycarpo[3], S. Ponce[49], D. Popov[7], S. Poslavskii[44], K. Prasanth[59], C. Prouve[81], D. Provenzano[32,j], V. Pugatch[53], G. Punzi[35,r], S. Qasim[51], Q. Q. Qian[6], W. Qian[7], N. Qin[4,b], S. Qu[4,b], R. Quagliani[49], R.I. Rabadan Trejo[57], J.H. Rademacker[55], M. Rama[35], M. Ramírez García[83], V. Ramos De Oliveira[70], M. Ramos Pernas[57], M.S. Rangel[3], F. Ratnikov[44], G. Raven[39], M. Rebollo De Miguel[48], F. Redi[30,h], J. Reich[55], F. Reiss[63], Z. Ren[7], P.K. Resmi[64], R. Ribatti[50], G. R. Ricart[15,12], D. Riccardi[35,q], S. Ricciardi[58], K. Richardson[65], M. Richardson-Slipper[59], K. Rinnert[61], P. Robbe[14,49], G. Robertson[60], E. Rodrigues[61], A. Rodriguez Alvarez[46], E. Rodriguez Fernandez[47], J.A. Rodriguez Lopez[75], E. Rodriguez Rodriguez[47], J. Roensch[19], A. Rogachev[44], A. Rogovskiy[58], D.L. Rolf[49], P. Roloff[49], V. Romanovskiy[66], A. Romero Vidal[47], G. Romolini[26], F. Ronchetti[50], T. Rong[6], M. Rotondo[28], S. R. Roy[22], M.S. Rudolph[69], M. Ruiz Diaz[22], R.A. Ruiz Fernandez[47], J. Ruiz Vidal[82,y], A. Ryzhikov[44], J. Ryzka[40], J. J. Saavedra-Arias[9], J.J. Saborido Silva[47], R. Sadek[15], N. Sagidova[44], D. Sahoo[77], N. Sahoo[54], B. Saitta[32,j], M. Salomoni[31,49,n], I. Sanderswood[48], R. Santacesaria[36], C. Santamarina Rios[47], M. Santimaria[28,49], L. Santoro [2], E. Santovetti[37], A. Saputi[26,49], D. Saranin[44], A. Sarnatskiy[78], G. Sarpis[59], M. Sarpis[63], C. Satriano[36,s], A. Satta[37], M. Saur[6], D. Savrina[44], H. Sazak[17], F. Sborzacchi[49,28], L.G. Scantlebury Smead[64], A. Scarabotto[19], S. Schael[17], S. Scherl[61], M. Schiller[60], H. Schindler[49], M. Schmelling[21], B. Schmidt[49], S. Schmitt[17], H. Schmitz[18], O. Schneider[50], A. Schopper[49], N. Schulte[19], S. Schulte[50], M.H. Schune[14], R. Schwemmer[49], G. Schwering[17], B. Sciascia[28], A. Sciuccati[49], I. Segal[76], S. Sellam[47], A. Semennikov[44], T. Senger[51], M. Senghi Soares[39], A. Sergi[29,l], N. Serra[51], L. Sestini[33], A. Seuthe[19], Y. Shang[6], D.M. Shangase[83], M. Shapkin[44], R. S. Sharma[69], I. Shchemerov[44], L. Shchutska[50], T. Shears[61], L. Shekhtman[44], Z. Shen[6], S. Sheng[5,7], V. Shevchenko[44], B. Shi[7], Q. Shi[7], Y. Shimizu[14], E. Shmanin[25], R. Shorkin[44], J.D. Shupperd[69], R. Silva Coutinho[69], G. Simi[33,o], S. Simone[24,g], N. Skidmore[57], T. Skwarnicki[69], M.W. Slater[54], J.C. Smallwood[64], E. Smith[65], K. Smith[68], M. Smith[62], A. Snoch[38], L. Soares Lavra[59], M.D. Sokoloff[66], F.J.P. Soler[60], A. Solomin[44,55], A. Solovev[44], I. Solovyev[44], N. S. Sommerfeld[18], R. Song[1], Y. Song[50], Y. Song[4,b], Y. S. Song[6], F.L. Souza De Almeida[69], B. Souza De Paula[3], E. Spadaro Norella[29,l], E. Spedicato[25], J.G. Speer[19], E. Spiridenkov[44], P. Spradlin[60], V. Sriskaran[49], F. Stagni[49], M. Stahl[49], S. Stahl[49], S. Stanislaus[64], E.N. Stein[49], O. Steinkamp[51], O. Stenyakin[44], H. Stevens[19], D. Strekalina[44], Y. Su[7], F. Suljik[64], J. Sun[32], L. Sun[74], D. Sundfeld[2], W. Sutcliffe[51], P.N. Swallow[54], K. Swientek[40], F. Swystun[56], A. Szabelski[42], T. Szumlak[40], Y. Tan[4,b], Y. Tang[74], M.D. Tat[64], A. Terentev[44], F. Terzuoli[35,u,49], F. Teubert[49], E. Thomas[49], D.J.D. Thompson[54], H. Tilquin[62],

V. Tisserand[11], S. T'Jampens[10], M. Tobin[5,49], L. Tomassetti[26,k], G. Tonani[30,m,49], X. Tong[6], D. Torres Machado[2], L. Toscano[19], D.Y. Tou[4,b], C. Trippl[45], G. Tuci[22], N. Tuning[38], L.H. Uecker[22], A. Ukleja[40], D.J. Unverzagt[22], B. Urbach[59], E. Ursov[44], A. Usachov[39], A. Ustyuzhanin[44], U. Uwer[22], V. Vagnoni[25], V. Valcarce Cadenas[47], G. Valenti[25], N. Valls Canudas[49], J. van Eldik[49], H. Van Hecke[68], E. van Herwijnen[62], C.B. Van Hulse[47,w], R. Van Laak[50], M. van Veghel[38], G. Vasquez[51], R. Vazquez Gomez[46], P. Vazquez Regueiro[47], C. Vázquez Sierra[47], S. Vecchi[26], J.J. Velthuis[55], M. Veltri[27,v], A. Venkateswaran[50], M. Verdoglia[32], M. Vesterinen[57], D. Vico Benet[64], P. V. Vidrier Villalba[46], M. Vieites Diaz[49], X. Vilasis-Cardona[45], E. Vilella Figueras[61], A. Villa[25], P. Vincent[16], F.C. Volle[54], D. vom Bruch[13], N. Voropaev[44], K. Vos[79], C. Vrahas[59], J. Wagner[19], J. Walsh[35], E.J. Walton[1,57], G. Wan[6], C. Wang[22], G. Wang[8], J. Wang[6], J. Wang[5], J. Wang[4,b], J. Wang[74], M. Wang[30], N. W. Wang[7], R. Wang[55], X. Wang[8], X. Wang[72], X. W. Wang[62], Y. Wang[6], Z. Wang[14], Z. Wang[4,b], Z. Wang[30], J.A. Ward[57,1], M. Waterlaat[49], N.K. Watson[54], D. Websdale[62], Y. Wei[6], J. Wendel[81], B.D.C. Westhenry[55], C. White[56], M. Whitehead[60], E. Whiter[54], A.R. Wiederhold[63], D. Wiedner[19], G. Wilkinson[64], M.K. Wilkinson[66], M. Williams[65], M. J. Williams[49], M.R.J. Williams[59], R. Williams[56], Z. Williams[55], F.F. Wilson[58], M. Winn[12], W. Wislicki[42], M. Witek[41], L. Witola[22], G. Wormser[14], S.A. Wotton[56], H. Wu[69], J. Wu[8], X. Wu[74], Y. Wu[6], Z. Wu[7], K. Wyllie[49], S. Xian[72], Z. Xiang[5], Y. Xie[8], A. Xu[35], J. Xu[7], L. Xu[4,b], L. Xu[4,b], M. Xu[57], Z. Xu[49], Z. Xu[7], Z. Xu[5], K. Yang[62], S. Yang[7], X. Yang[6], Y. Yang[29,l], Z. Yang[6], V. Yeroshenko[14], H. Yeung[63], H. Yin[8], C. Y. Yu[6], J. Yu[71], X. Yuan[5], Y Yuan[5,7], E. Zaffaroni[50], M. Zavertyaev[21], M. Zdybal[41], F. Zenesini[25,i], C. Zeng[5,7], M. Zeng[4,b], C. Zhang[6], D. Zhang[8], J. Zhang[7], L. Zhang[4,b], S. Zhang[71], S. Zhang[64], Y. Zhang[6], Y. Z. Zhang[4,b], Z. Zhang[4,b], Y. Zhao[22], A. Zharkova[44], A. Zhelezov[22], S. Z. Zheng[6], X. Z. Zheng[4,b], Y. Zheng[7], T. Zhou[6], X. Zhou[8], Y. Zhou[7], V. Zhovkovska[57], L. Z. Zhu[7], X. Zhu[4,b], X. Zhu[8], V. Zhukov[17], J. Zhuo[48], Q. Zou[5,7], D. Zuliani[33,o], G. Zunica[50].

[1]*School of Physics and Astronomy, Monash University, Melbourne, Australia*
[2]*Centro Brasileiro de Pesquisas Físicas (CBPF), Rio de Janeiro, Brazil*
[3]*Universidade Federal do Rio de Janeiro (UFRJ), Rio de Janeiro, Brazil*
[4]*Department of Engineering Physics, Tsinghua University, Beijing, China, Beijing, China*
[5]*Institute Of High Energy Physics (IHEP), Beijing, China*
[6]*School of Physics State Key Laboratory of Nuclear Physics and Technology, Peking University, Beijing, China*
[7]*University of Chinese Academy of Sciences, Beijing, China*
[8]*Institute of Particle Physics, Central China Normal University, Wuhan, Hubei, China*
[9]*Consejo Nacional de Rectores (CONARE), San Jose, Costa Rica*
[10]*Université Savoie Mont Blanc, CNRS, IN2P3-LAPP, Annecy, France*
[11]*Université Clermont Auvergne, CNRS/IN2P3, LPC, Clermont-Ferrand, France*
[12]*Département de Physique Nucléaire (DPhN), Gif-Sur-Yvette, France*
[13]*Aix Marseille Univ, CNRS/IN2P3, CPPM, Marseille, France*
[14]*Université Paris-Saclay, CNRS/IN2P3, IJCLab, Orsay, France*
[15]*Laboratoire Leprince-Ringuet, CNRS/IN2P3, Ecole Polytechnique, Institut Polytechnique de Paris, Palaiseau, France*
[16]*LPNHE, Sorbonne Université, Paris Diderot Sorbonne Paris Cité, CNRS/IN2P3, Paris, France*
[17]*I. Physikalisches Institut, RWTH Aachen University, Aachen, Germany*
[18]*Universität Bonn - Helmholtz-Institut für Strahlen und Kernphysik, Bonn, Germany*
[19]*Fakultät Physik, Technische Universität Dortmund, Dortmund, Germany*
[20]*Physikalisches Institut, Albert-Ludwigs-Universität Freiburg, Freiburg, Germany*

[21]*Max-Planck-Institut für Kernphysik (MPIK), Heidelberg, Germany*
[22]*Physikalisches Institut, Ruprecht-Karls-Universität Heidelberg, Heidelberg, Germany*
[23]*School of Physics, University College Dublin, Dublin, Ireland*
[24]*INFN Sezione di Bari, Bari, Italy*
[25]*INFN Sezione di Bologna, Bologna, Italy*
[26]*INFN Sezione di Ferrara, Ferrara, Italy*
[27]*INFN Sezione di Firenze, Firenze, Italy*
[28]*INFN Laboratori Nazionali di Frascati, Frascati, Italy*
[29]*INFN Sezione di Genova, Genova, Italy*
[30]*INFN Sezione di Milano, Milano, Italy*
[31]*INFN Sezione di Milano-Bicocca, Milano, Italy*
[32]*INFN Sezione di Cagliari, Monserrato, Italy*
[33]*INFN Sezione di Padova, Padova, Italy*
[34]*INFN Sezione di Perugia, Perugia, Italy*
[35]*INFN Sezione di Pisa, Pisa, Italy*
[36]*INFN Sezione di Roma La Sapienza, Roma, Italy*
[37]*INFN Sezione di Roma Tor Vergata, Roma, Italy*
[38]*Nikhef National Institute for Subatomic Physics, Amsterdam, Netherlands*
[39]*Nikhef National Institute for Subatomic Physics and VU University Amsterdam, Amsterdam, Netherlands*
[40]*AGH - University of Krakow, Faculty of Physics and Applied Computer Science, Kraków, Poland*
[41]*Henryk Niewodniczanski Institute of Nuclear Physics Polish Academy of Sciences, Kraków, Poland*
[42]*National Center for Nuclear Research (NCBJ), Warsaw, Poland*
[43]*Horia Hulubei National Institute of Physics and Nuclear Engineering, Bucharest-Magurele, Romania*
[44]*Affiliated with an institute covered by a cooperation agreement with CERN*
[45]*DS4DS, La Salle, Universitat Ramon Llull, Barcelona, Spain*
[46]*ICCUB, Universitat de Barcelona, Barcelona, Spain*
[47]*Instituto Galego de Física de Altas Enerxías (IGFAE), Universidade de Santiago de Compostela, Santiago de Compostela, Spain*
[48]*Instituto de Fisica Corpuscular, Centro Mixto Universidad de Valencia - CSIC, Valencia, Spain*
[49]*European Organization for Nuclear Research (CERN), Geneva, Switzerland*
[50]*Institute of Physics, Ecole Polytechnique Fédérale de Lausanne (EPFL), Lausanne, Switzerland*
[51]*Physik-Institut, Universität Zürich, Zürich, Switzerland*
[52]*NSC Kharkiv Institute of Physics and Technology (NSC KIPT), Kharkiv, Ukraine*
[53]*Institute for Nuclear Research of the National Academy of Sciences (KINR), Kyiv, Ukraine*
[54]*School of Physics and Astronomy, University of Birmingham, Birmingham, United Kingdom*
[55]*H.H. Wills Physics Laboratory, University of Bristol, Bristol, United Kingdom*
[56]*Cavendish Laboratory, University of Cambridge, Cambridge, United Kingdom*
[57]*Department of Physics, University of Warwick, Coventry, United Kingdom*
[58]*STFC Rutherford Appleton Laboratory, Didcot, United Kingdom*
[59]*School of Physics and Astronomy, University of Edinburgh, Edinburgh, United Kingdom*
[60]*School of Physics and Astronomy, University of Glasgow, Glasgow, United Kingdom*
[61]*Oliver Lodge Laboratory, University of Liverpool, Liverpool, United Kingdom*
[62]*Imperial College London, London, United Kingdom*
[63]*Department of Physics and Astronomy, University of Manchester, Manchester, United Kingdom*
[64]*Department of Physics, University of Oxford, Oxford, United Kingdom*
[65]*Massachusetts Institute of Technology, Cambridge, MA, United States*
[66]*University of Cincinnati, Cincinnati, OH, United States*
[67]*University of Maryland, College Park, MD, United States*
[68]*Los Alamos National Laboratory (LANL), Los Alamos, NM, United States*
[69]*Syracuse University, Syracuse, NY, United States*
[70]*Pontifícia Universidade Católica do Rio de Janeiro (PUC-Rio), Rio de Janeiro, Brazil, associated to* [3]
[71]*School of Physics and Electronics, Hunan University, Changsha City, China, associated to* [8]
[72]*Guangdong Provincial Key Laboratory of Nuclear Science, Guangdong-Hong Kong Joint Laboratory of Quantum Matter, Institute of Quantum Matter, South China Normal University, Guangzhou, China, associated to* [4]

[73] Lanzhou University, Lanzhou, China, associated to [5]
[74] School of Physics and Technology, Wuhan University, Wuhan, China, associated to [4]
[75] Departamento de Fisica , Universidad Nacional de Colombia, Bogota, Colombia, associated to [16]
[76] Ruhr Universitaet Bochum, Fakultaet f. Physik und Astronomie, Bochum, Germany, associated to [19]
[77] Eotvos Lorand University, Budapest, Hungary, associated to [49]
[78] Van Swinderen Institute, University of Groningen, Groningen, Netherlands, associated to [38]
[79] Universiteit Maastricht, Maastricht, Netherlands, associated to [38]
[80] Tadeusz Kosciuszko Cracow University of Technology, Cracow, Poland, associated to [41]
[81] Universidade da Coruña, A Coruña, Spain, associated to [45]
[82] Department of Physics and Astronomy, Uppsala University, Uppsala, Sweden, associated to [60]
[83] University of Michigan, Ann Arbor, MI, United States, associated to [69]

[a] Centro Federal de Educacão Tecnológica Celso Suckow da Fonseca, Rio De Janeiro, Brazil
[b] Center for High Energy Physics, Tsinghua University, Beijing, China
[c] Hangzhou Institute for Advanced Study, UCAS, Hangzhou, China
[d] School of Physics and Electronics, Henan University , Kaifeng, China
[e] LIP6, Sorbonne Université, Paris, France
[f] Universidad Nacional Autónoma de Honduras, Tegucigalpa, Honduras
[g] Università di Bari, Bari, Italy
[h] Università di Bergamo, Bergamo, Italy
[i] Università di Bologna, Bologna, Italy
[j] Università di Cagliari, Cagliari, Italy
[k] Università di Ferrara, Ferrara, Italy
[l] Università di Genova, Genova, Italy
[m] Università degli Studi di Milano, Milano, Italy
[n] Università degli Studi di Milano-Bicocca, Milano, Italy
[o] Università di Padova, Padova, Italy
[p] Università di Perugia, Perugia, Italy
[q] Scuola Normale Superiore, Pisa, Italy
[r] Università di Pisa, Pisa, Italy
[s] Università della Basilicata, Potenza, Italy
[t] Università di Roma Tor Vergata, Roma, Italy
[u] Università di Siena, Siena, Italy
[v] Università di Urbino, Urbino, Italy
[w] Universidad de Alcalá, Alcalá de Henares , Spain
[x] Facultad de Ciencias Fisicas, Madrid, Spain
[y] Department of Physics/Division of Particle Physics, Lund, Sweden

[†] Deceased